Supporting Information

Moeller et al. 10.1073/pnas.1419136111

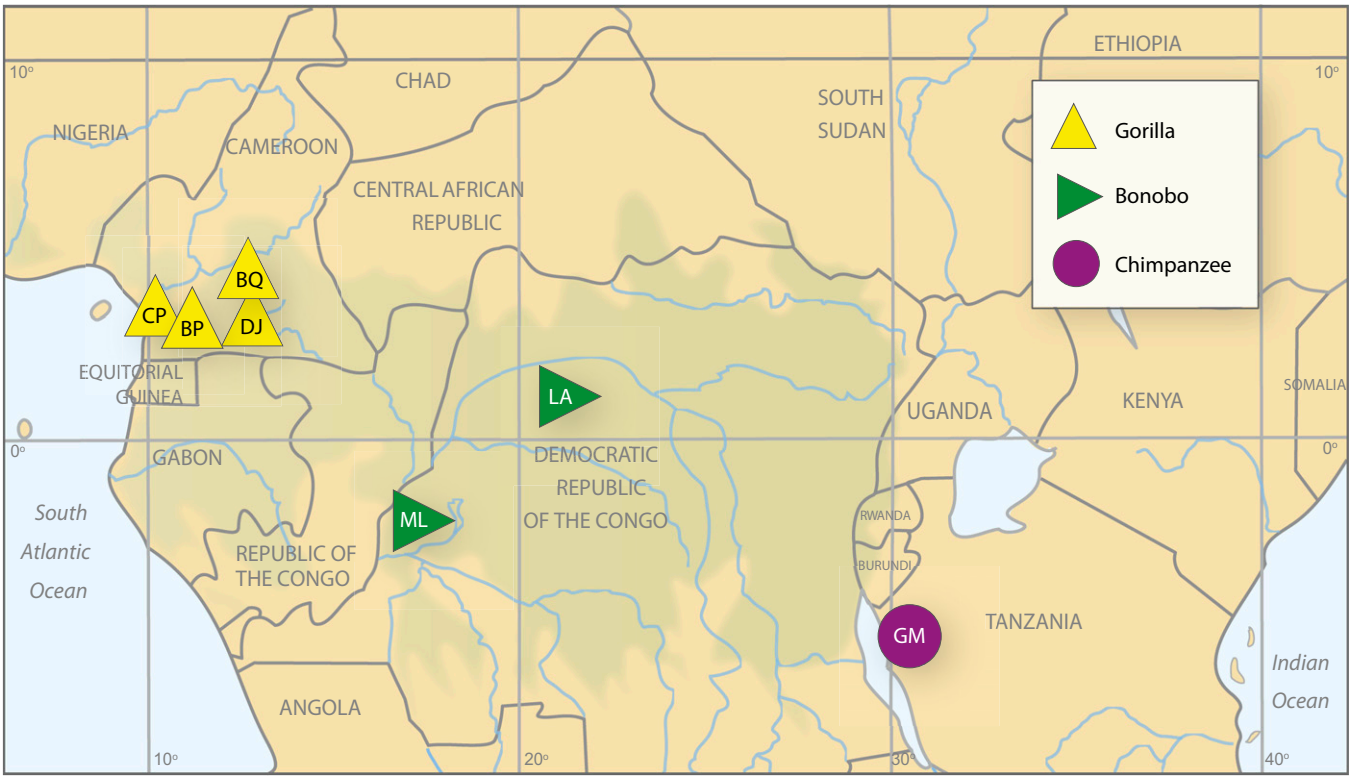

Fig. S1. Map of African ape sampling locations. Sites from which microbiomes of wild ape populations were sampled are shown. Yellow triangles mark sites where gorillas were sampled (CP, Campo Ma'an; BP, Bipindi; BQ, Belgique; DJ, Doujum), green triangles indicate sites where bonobos were sampled (LA, Lomako; ML, Malebo), and the purple circle denotes the site where chimpanzees were sampled (GM, Gombe).

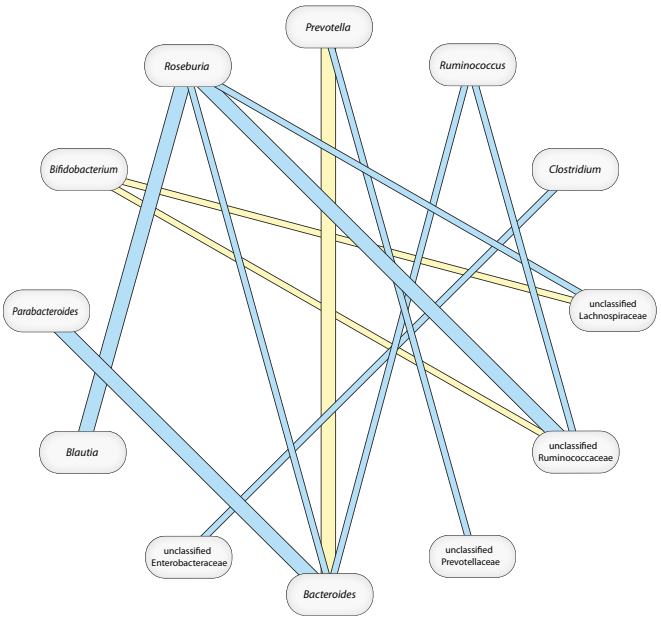

Fig. S2. Consistent bacterial co-occurrence patterns within the microbiomes of humans and African apes. Bacterial taxa are connected by blue and yellow lines, which indicate positive and negative Pearson correlations between the relative abundances of taxa. Only correlations detected within each sampled host species are shown. Correlations with absolute values 0.3–0.4 in each sampled host species are denoted by narrow lines; correlations with absolute values >0.4 in each sampled host species, by wider lines.

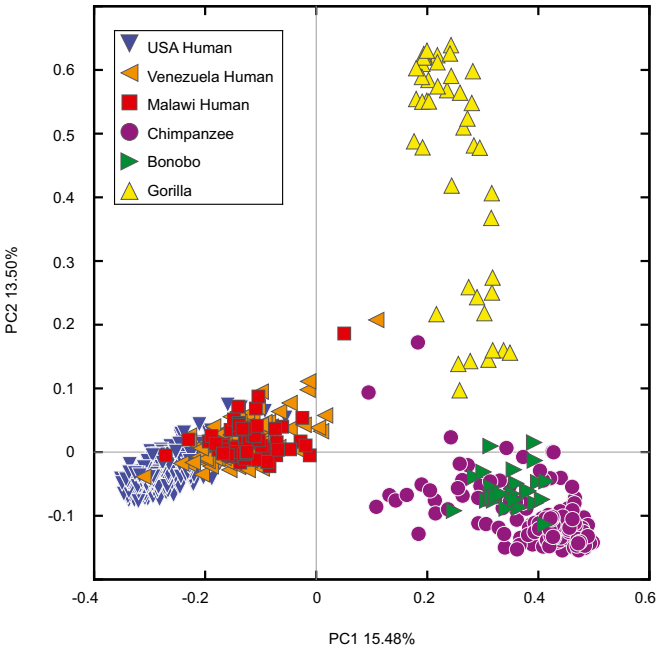

Fig. S3. OTU-level beta diversity among samples. Principal coordinates plots of BCDs among the relative abundances of OTUs reveal separation of human and ape populations. Colored shapes correspond to individual samples recovered from host populations, as indicated in the key.

Fig. S4. Compositional shifts in the microbiome differentiate human populations. Listed above and below branches are the most parsimonious increases and decreases, respectively, in relative abundances of microbial taxa that explain the present-day variation among microbiomes of humans from the United States, Venezuela, and Malawi. The tree is not drawn to a time scale, and the relationships among human populations is represented as a polytomy.

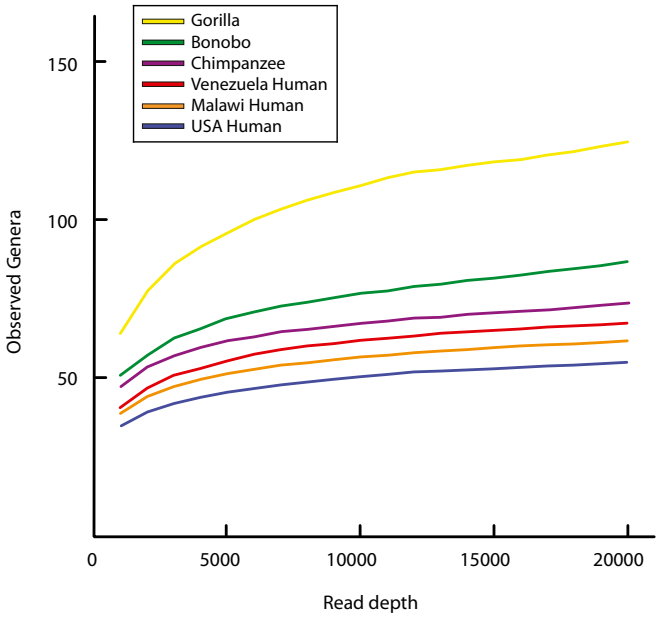

Fig. S5. Rarefaction curves of genus-level bacterial diversity. Rarefaction lines correspond to average numbers of microbial genera recovered from individuals of different host species and human populations across sequencing depths. Ten rarefactions were performed for every 1,000-sequence sampling increment.

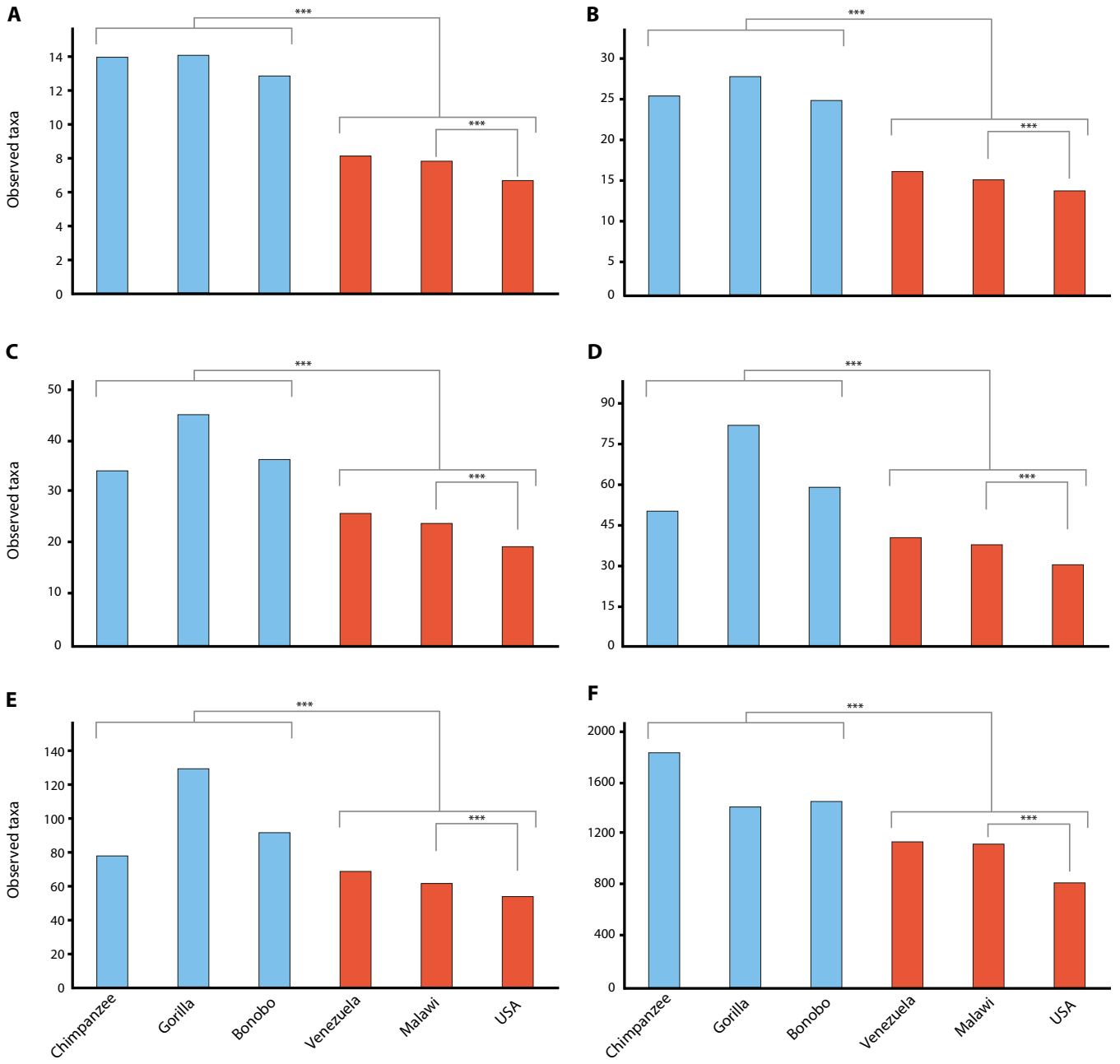

Fig. S6. Within-individual diversity across taxonomic levels. Levels of microbial diversity recovered from individuals of different host species and human populations at a sequencing depth of 20,000 reads. Shown are average numbers of microbial taxa recovered at the level of phylum (*A*) class (*B*) order (*C*), family (*D*), genus (*E*), and 97% out (*F*).

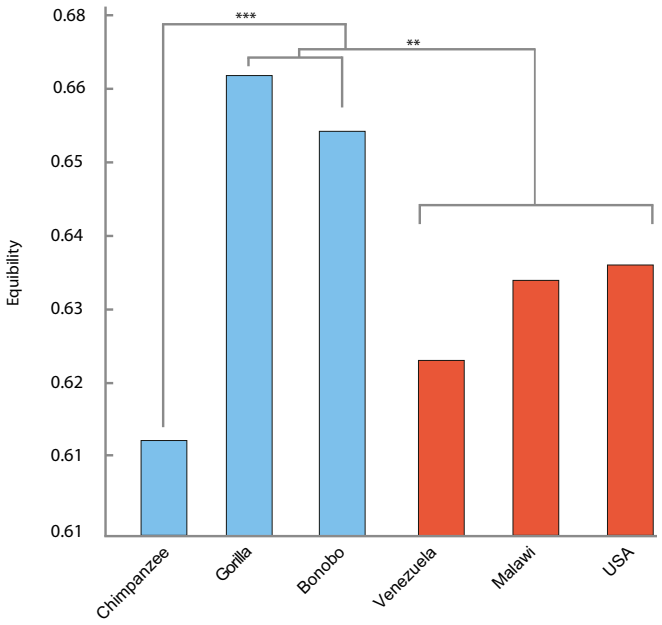

Fig. S7. Evenness of genus-level diversity within individuals. Mean equibility values of individual microbiomes across host populations and species are shown. Asterisks denote the statistical significance of differences between means (**$P < 0.01$; ***$P < 0.001$).

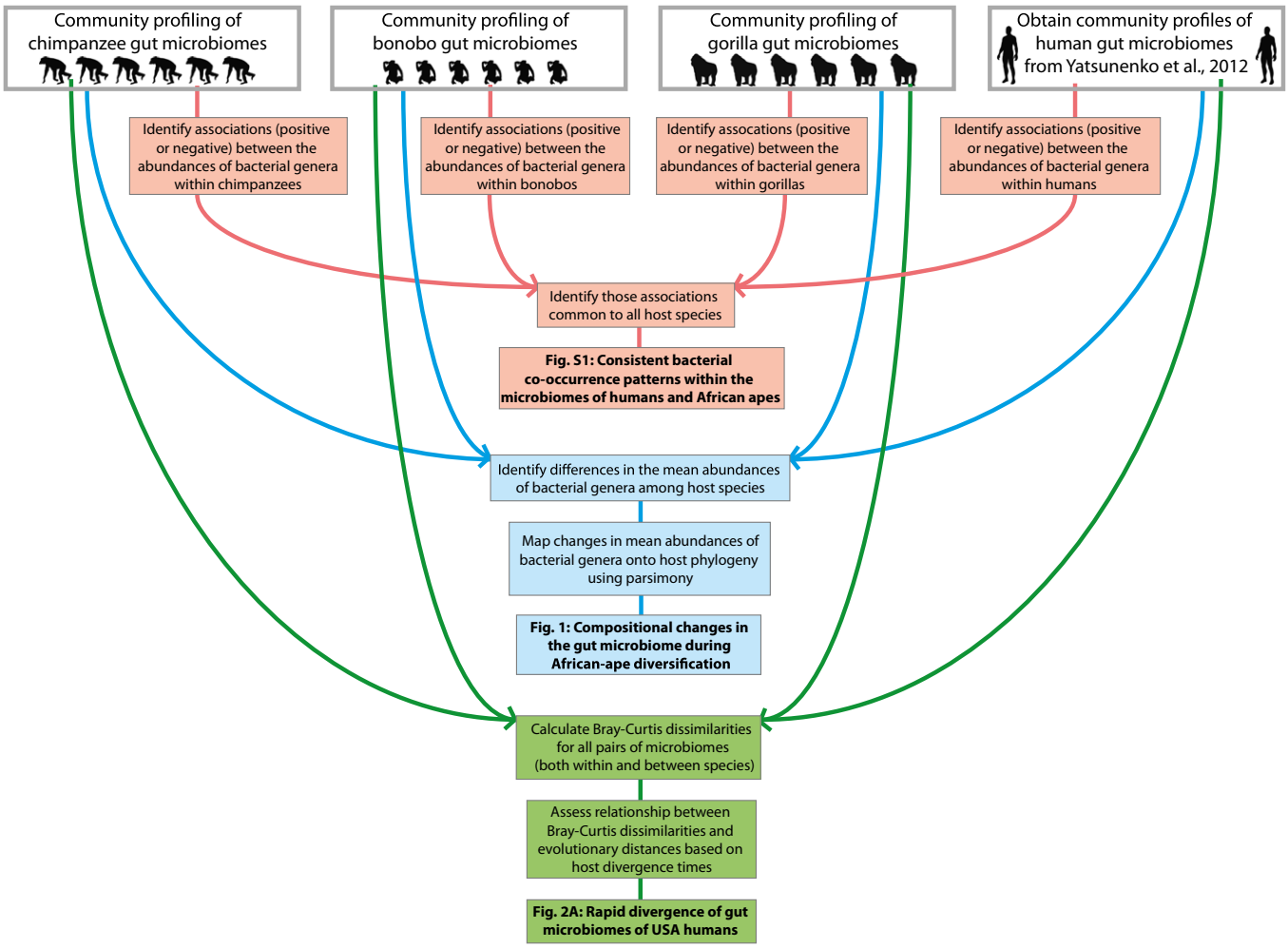

Fig. S8. Summary of evolutionary analyses of human and ape microbiomes. The flowchart depicts analyses used to identify conserved and variable features of human and ape microbiomes. Each box contains either a step of an analysis or a result (in bold type), and arrows connecting boxes indicate the order in which steps were performed.

Other Supporting Information Files

Table S1 (DOCX)